Chinese Journal of Chemical Engineering, **16**(1) 135—142 (2008)

Elementary Flux Mode Analysis for Optimized Ethanol Yield in Anaerobic Fermentation of Glucose with *Saccharomyces cerevisiae**

XU Xiaojing (许晓菁)**, **CAO Limin** (曹利民) **and CHEN Xun** (陈询)
Department of Biochemical Engineering, School of Chemical Engineering & Technology, Tianjin University, Tianjin 300072, China

Abstract Elementary flux mode (EFM) analysis was used in the metabolic analysis of central carbon metabolism in *Saccharomyces cerevisiae* based on constructed cellular network. Calculated from the metabolic model, the ethanol-producing pathway No. 37 furthest converts the substrate into ethanol among the 78 elementary flux modes. The in silico metabolic phenotypes predicted based on this analysis fit well with the fermentation performance of the engineered strains, KAM3 and KAM11, which confirmed that EFM analysis is valid to direct the construction of *Saccharomyces cerevisiae* engineered strains, to increase the ethanol yield.
Keywords elementary flux mode analysis, metabolic phenotype, redox balance, *Saccharomyces cerevisiae*, ethanol

1 INTRODUCTION

Efficient substrate utilization and elimination or reduction of byproduct formation are key factors for the economy of the ethanol industry. Glycerol is a major byproduct in anaerobic ethanol fermentation and consumes up to 4% of the total carbon source in the medium. The main physiological roles of glycerol formation are osmoregulation and maintaining redox balance [1-4]. To achieve maximum conversion rate of glucose to ethanol, many attempts have been made to impair glycerol synthesis and redirect carbon flux from glycerol formation toward ethanol production. Some strain improvement strategies focused on the genetic modification of the glycerol synthesis pathway by deleting the *GPD1* and *GPD2* genes, encoding two isoenzymes of NAD^+-dependent glycerol 3-phosphate dehydrogenase [5-7]. Other studies focused on regulating redox balance in ammonia metabolism by overexpressing the *GLT1* and *GLN1* genes, encoding glutamate synthase and glutamine synthase, respectively [8-10]. Recently, the Fps1p channel protein, which regulates glycerol export by facilitated diffusion, has drawn new attention to the field [11-14]. Glycerol formed in the *fps1Δ* strain cannot be exported through the Fps1p channel and, as a consequence, the buildup of a high level of intracellular glycerol will then inhibit the formation of glycerol [15].

However, gene modifications of individual metabolic pathways often produce no satisfactory results on account of the complexity of metabolic control mechanism. To bring about new insight into the biological processes at the systems level, global cellular metabolic networks have recently been reconstructed for *S. cerevisiae* [16-18]. Elementary flux mode (EFM) is one of mathematical tools for metabolic pathway analysis. It has been applied to predict the optimal conversion rate and systemically analyze balanced metabolic and cellular network engineering [19-21]. Based on EFM analysis, the gene modification strategies have been synthetically designed from the "pathway point " of view other than the viewpoint of separate reactions [22-26].

Currently, there is no report about the application of EFM in *S. cerevisiae* fermentation to optimize ethanol production. To study the feasibility of EFM analysis in *S. cerevisiae*, the authors constructed a simplified metabolic model based on the global cellular metabolic networks of *S. cerevisiae*, and applied EFM analysis, to display the metabolic phenotypes of genetically engineered strains KAM3 (*fps1Δ*) and KAM11 (*fps1Δ PGK1p-GLT1*). The ethanol yields for different metabolic pathways were predicted and then compared with the experimental results.

2 MATERIALS AND METHODS

2.1 Strains

Strains used in this study are listed in Table 1. KAM2 is a haploid progeny of an industrial diploid strain (Angel Yeast Co. Ltd.). The engineered strains KAM3 and KAM11 are derivatives of KAM2.

Table 1 Strains used in this study

Name	Gene type description	Source
KAM2	*Mat α ura3*	Ref.[27]
KAM3	*Mat α ura3 fps1Δ*:: REPEAT	Ref.[27]
KAM11	*Mat α ura3 fps1Δ*:: REPEAT *PGK1p-GLT1*	Ref.[27]

2.2 Batch fermentation

Batch fermentation was carried out at 30°C and 200r·min^{-1} in 200 ml in-house-manufactured bioreactors sealed with screw caps. The working volume of the bioreactors was 150 ml and a defined medium [glucose 20 g·L^{-1}, yeast nitrogen base (YNB) with ammonium sulfate 6.7 g·L^{-1}, adenine 100 mg·L^{-1}, methionine 100 mg·L^{-1}, lysine 150 mg·L^{-1}] was used

Received 2007-04-19, accepted 2007-08-11.
* Supported by the National Natural Science Foundation of China (No.2002AA647040).
** To whom correspondence should be addressed. E-mail: susy8470@yahoo.com.cn

as the fermentation medium. An overnight preculture was inoculated into the bioreactors to reach an initial OD_{660} 1.0. CO_2 formed under anaerobic cultivations was gathered into exhaust collectors through pipes. The pH was maintained at 5.0 by addition of 2 mol·L^{-1} KOH. All experiments were performed in duplicate, and the results were the means of the duplicate trials.

2.3 Analysis methods

The optical density of the culture was determined at 660nm with a spectrophotometer (CE2502 BIOQUEST, BRITAIN). To determine cell dry mass, 10ml fermentation broth was centrifuged at 3800 r·min^{-1} for 10min in preweighed tubes, the supernatant was decanted, and pellets were dried at 65°C until constant.

The content of glucose, ethanol, glycerol, acetic acid, and pyruvic acid in the fermentation broth was determined by HPLC and GC, as described in Ref. [27].

2.4 Real-time reverse transcript-polymerase chain reaction

Total RNA isolation from yeast cells was carried out by standard procedure. Total RNA of 5 μg was digested with RNase-free DNase I (Promega) for 35 min at 37°C to remove residual DNA, and 2.5 μg of the Dnase-treated RNA was reverse transcribed into cDNA using Superscript II reverse transcriptase (Invitrogen).

The real-time reverse transcript-polymerase chain reaction (RT-PCR) reactions were carried out in a 20μl volume using LightCycler-FastStart DNA Master SYBR Green I Kit (Roche Applied Science). All primers used in this study were designed with the Primer Premier 5.0 software (Premier, Canada) and synthesized at Invitrogen. The forward and reverse primers for RT-PCR analysis of the *GLT1* gene were *GLT1*-F (5′-ggattaagccttgtccacca-3′) and *GLT1*-R (5′-ccatacatcaataacccaccac-3′), respectively. Primers for the housekeeping gene *ACT1* were *ACT1*-F (5′-gaagctccaatgaaccctaaat-3′) and *ACT1*-R (5′-accggaagagtacaaggacaaa-3′), respectively. Thermocycler conditions for all reactions were: 95°C for 10min, followed by 40 cycles of 95°C for 15 s, 58°C for 1min, 72°C for 15 s, and 76°C for 3 s.

2.5 Depiction of metabolic network model for *S. cerevisiae* strains

A simplified stoichiometric model of the central carbon metabolism of *S. cerevisiae* (see Appendix and Fig. 1) was constructed. The metabolic network was composed of 35 different reactions, which existed in the glycolysis, pentose phosphate pathway, citric acid cycle, and ammonium assimilation pathway [17, 28–30]. Two cellular compartments, cytosol and mitochondria and extracellular space were applied to ideally depict the redox balance. The biomass synthesis equation was achieved by drain of metabolite precursors into the biomass pathway (R1) [29]. One important group

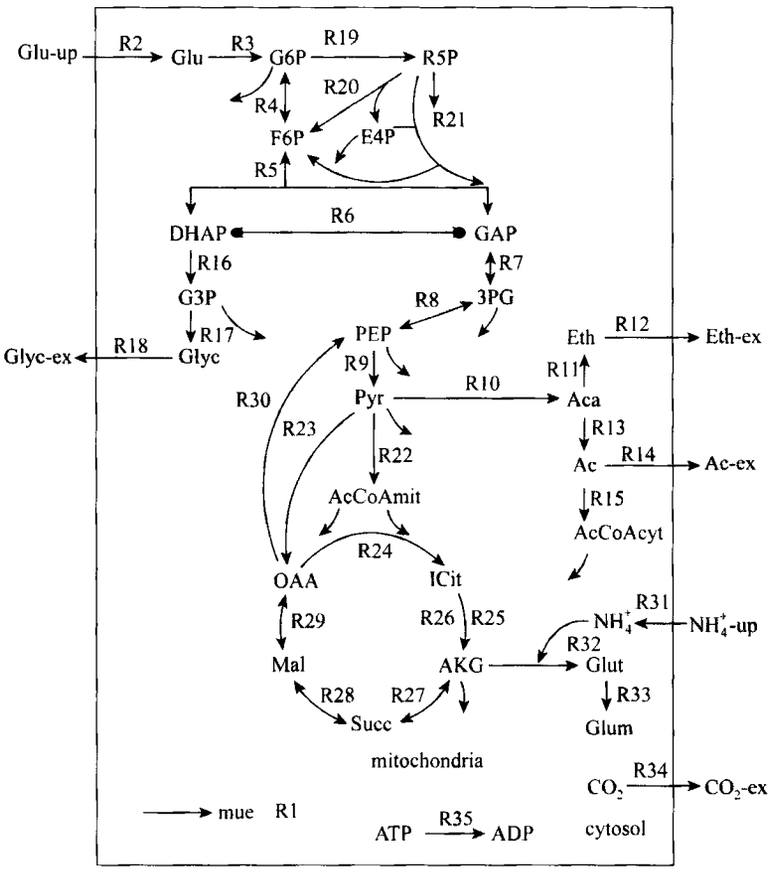

Figure 1 Metabolic network model for *S. cerevisiae*

of isoenzymes of isocitrate dehydrogenase (Idh1, Idp1 and Idp2) was localized in two different compartments, which catalyze the corresponding reactions in the model (R25 and R26). The reaction induced by Idp2 was neglected because of its inactive growth on glucose. The channel protein Fps1p controlled the export of glycerol from the cell in the model (R18). In the ammonium assimilation pathway glutamate was synthesized by expression of *GLT1* and *GLN1* in two coupled pathways in the model (R31, R32 and R33). Moreover, the necessary ATP consumption was used for maintenance and futile cycles (R35).

The EFM pathways in the metabolic network were calculated by Fluxanalyzer 5.3 combined with Matlab [26].

3 RESULTS AND DISCUSSION

3.1 Metabolic phenotype prediction by EFM pathway analysis

Metabolic phenotypes were predicted according to EFM analysis for different strains. EFM pathways were calculated based on different strains cultured on glucose anaerobically (Table 2). The gene deletion or overexpression could have either a positive or negative effect on growth phenotypes [31]. Essential genes and essential reactions in the EFM pathways could not be deleted.

Table 2 EFMs of different reactions analyzed

Reaction condition	All EFMs	Ethanol	Glycerol	Glutamate	Acetate	Biomass
EFMs	78	9	33	34	9	22
remove R18	38	5	0	5	5	8

In silico deletion of *FPS1* and overexpression of *GLT1* in the reference strain were assessed by EFM analysis. The *fps1Δ* mutant phenotype was predicted to be viable, but exhibit a slow growth phenotype because of the buildup of high intracellular glycerol concentration. On the other hand, the maximum specific growth rate was predicted to increase by overexpression of *GLT1* based on EFM analysis. These predictions were in good agreement with the experimental data reported previously [4, 9, 25, 32].

3.2 The calculated mode yields by EFM pathway analysis

Among the 33 glycerol-producing modes, the highest glycerol yield was obtained from EFM pathway No.1 (Table 3 and Fig. 2). The theoretical ethanol yield with zero biomass formation was reflected in EFM pathway No.37 (Table 4 and Fig. 3). In view of the ethanol-producing/glycerol-coproducing modes, the predicted higher ethanol yield, which was on account of the redirection of carbon flux from glycerol to ethanol by impairing glycerol synthesis, largely supported the pathway design strategies.

Among the 34 glutamate-producing modes, the

Table 3 Description of the glycerol-producing pathway yields

EFM pathway No.	Mode stoichiometry	Glycerol yield①/g·g^{-1}
1	2 Glu-up=2 Glyc-ex + 1 CO_2	0.511
26	3 Glu-up=2 Glyc-ex + 6 CO_2 + 3 Ac-ex	0.341
31	3 Glu-up + 1.5 NH_4^+ =2 Glyc-ex + 4.5 CO_2 + 1.5 Glut	0.341

① Based on grams of glucose consumed.

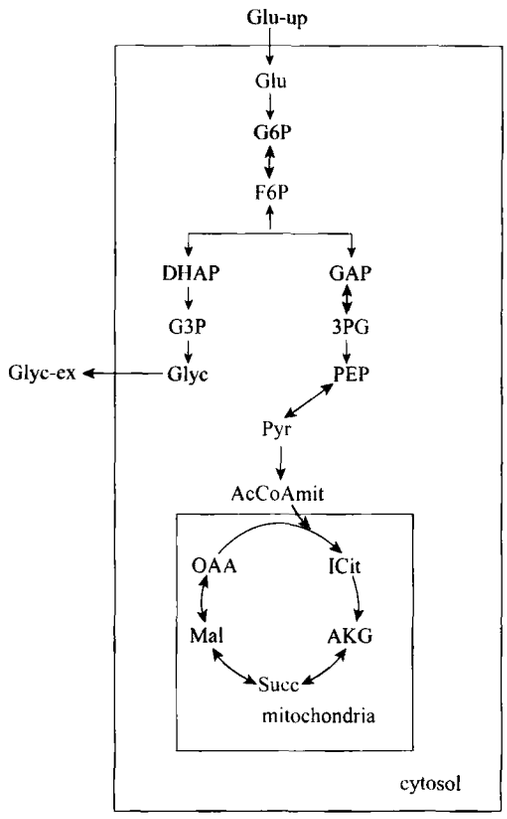

Figure 2 Graphical representation of the optimal producing-glycerol EFM

Table 4 Description of the ethanol-producing pathway yields

EFM pathway No.	Mode stoichiometry	Ethanol yield①/g·g^{-1}
25	1 Glu-up=1 Eth-ex + 1 CO_2 + 1 Glyc-ex	0.256
27	3 Glu-up=3 Eth-ex + 6 CO_2 + 2 Glyc-ex	0.256
35	3 Glu-up=5 Eth-ex + 8 CO_2	0.426
37	1 Glu-up=2 Eth-ex + 2 CO_2	0.511 (theoretical yield)

① Based on grams of glucose consumed.

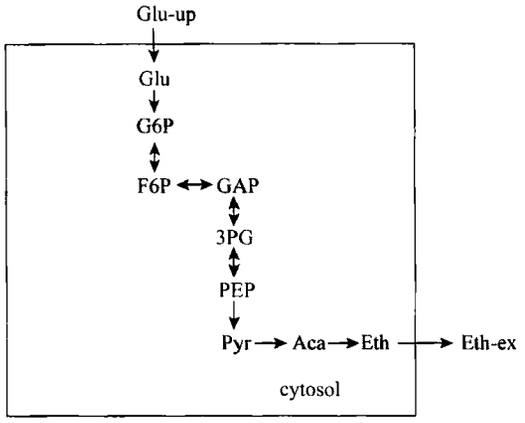

Figure 3 Graphical representation of the optimal ethanol-producing EFM

highest glutamate conversion rate was present in the EFM pathway No.58, which involved the tricarboxylic acid (TCA) cycle (Table 5 and Fig. 4). In EFM No.1, which included the pentose phosphate pathway (PPP), the glycerol yield was increased by overexpression of *GLT1* concomitantly with more consumption of ATP and NADH in the cytosol. The ethanol yield was also increased, resulting from more consumption of ATP. The ethanol yield was further increased because of the combined effects of gene deletion (*FPS1*) and gene overexpression (*GLT1*).

According to the results of the EFM analysis, the acetate yield was predicted to decrease in the corresponding pathways, which were inhibited by surplus NADH, when the glycerol production capacity was hampered. The maximum conversion rate of glucose to acetate was 66.67% among the nine acetate-producing modes (Table 6 and Fig. 5). The generation of cofactors, such as, NADH and NADPH in the cytosol, was

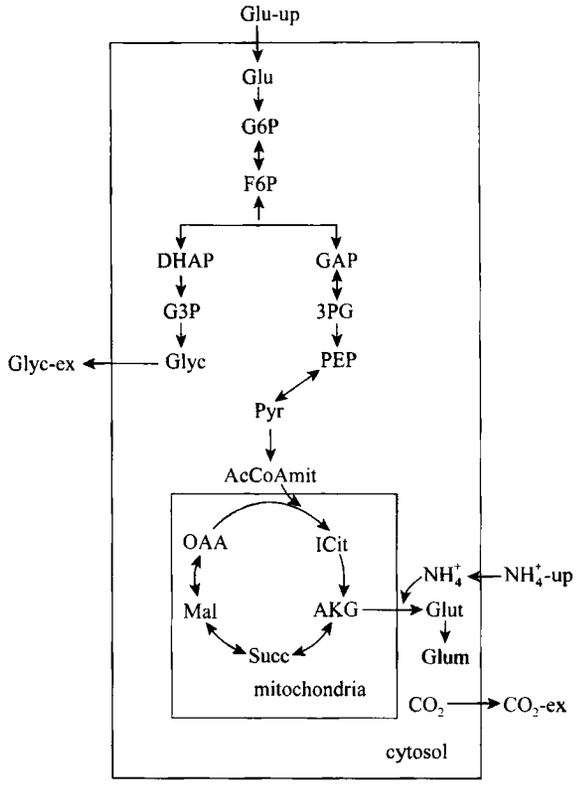

Figure 4 Graphical representation of the optimal glutamate-producing EFM

simultaneously accompanied by acetate formation. Moreover, the acetate was converted into Acetyl-CoA in either cytosol or mitochondria and, therefore, when the acetate yield decreased, less biomass was produced because of reduced availability of cofactors and metabolic precursors such as acetyl-CoA. Considering precursor metabolites and cofactors directed into the

Table 5 Description of the glutamate-producing pathway yields

EFM pathway No.	Mode stoichiometry	Glutamate yield[①]/g·g^{-1}
1	2 Glu-up + 1 ATP + 1 NH_4^+-up + 1 NAD$^+$mit + 1 NADHcyt=2 Glyc-ex +1 ADP + 1 NADHmit + 1 NAD$^+$cyt + 1 CO_2-ex + 1 Glut	0.409
58	1.5 Glu-up + 1 ATP + 1 NH_4^+-up + 2 NADHmit + 1 $FADH_2$ + 1 CO_2=1 Eth-ex + 1 ADP + 1 FAD + 2 NAD$^+$mit + 1 Glut	0.545
73	3 Glu-up + 4 ATP + 1 NH_4^+-up + 2 CO_2 + 1 $FADH_2$ + 2 NADHmit + 1 NAD$^+$cyt= 2 Glyc-ex + 2 Ac-ex + 1 FAD+ 4 ADP + 2 NAD+mit + 1 NADHcyt + 1 Glut	0.273

① Based on grams of glucose consumed.

Table 6 Description of the acetate-producing pathway yields

EFM pathway No.	Mode stoichiometry	Acetate yield[①]/g·g^{-1}
24	1 Glu-up + 1 NADP$^+$cyt=1 Glyc-ex + 1 Ac-ex + 1 NADPHcyt + 1 CO_2-ex	0.333
26	3 Glu-up + 1 ADP + 1 NAD$^+$cyt + 9 NADP$^+$cyt =2 Glyc-ex + 3 Ac-ex + 6 CO_2-ex + 1 ATP + 1 NADHcyt + 9 NADPHcyt	0.333
38	1 Glu-up + 2 ADP + 2 NAD$^+$cyt + 2 NADP$^+$cyt =2 Ac-ex + 2 CO_2-ex + 2 ATP +2 NADHcyt + 2NADPHcyt	0.667
74	3 Glu-up + 4 ATP + 1 NH_4^+-up + 2 CO_2 + 1 $FADH_2$ + 1 NADHcyt + 1 NADP$^+$cyt=2 Glyc-ex + 2 Ac-ex + 1 FAD+ 4 ADP + 1 NAD$^+$cyt + 1 NADPHcyt + 1 Glut	0.222

① Based on grams of glucose consumed.

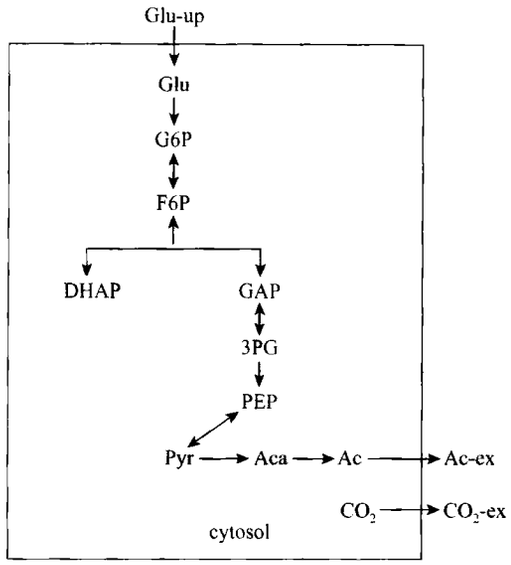

Figure 5 Graphical representation of the optimal acetate-producing EFM

biomass synthesis, biomass yields were calculated under anaerobic fermentation conditions (Table 7). Consistent with the previous studies [6, 23, 33], the maximum biomass yield based on grams of glucose consumed ($0.187 g \cdot g^{-1}$) was achieved in the EFM pathway No.68 (Fig. 6). Different *S. cerevisiae* strains had analogical maximum biomass yields in EFM analysis indicating that the central carbon metabolism of *S. cerevisiae* could be robustness.

3.3 The experimental results of anaerobic fermentation

To verify that *GLT1* was overexpressed in strain KAM11, the expression level of *GLT1* in strains KAM3 and KAM11 was investigated by real-time RT-PCR. As shown in Fig. 7, the expression of *GLT1* in strain KAM11 was 11.8 times that in strain KAM3, demonstrating that the *GLT1* gene in strain KAM11 was indeed overexpressed, as desired.

The results of anaerobic batch cultivations showed that the maximum specific growth rate of the two engineered yeast strains was slightly lower than that of strain KAM2 (Table 8). Overexpression of *GLT1* in strain KAM11 increased the maximum specific growth rate to some extent (Fig.8). The ethanol volumetric productivity of the three strains was measured. As shown in Table 8, although the ethanol volumetric productivity of strain KAM11 increased by 6.9% compared to strain KAM2, no significant differences were detected between KAM2 and KAM3. The experimental biomass yields were somewhat less than

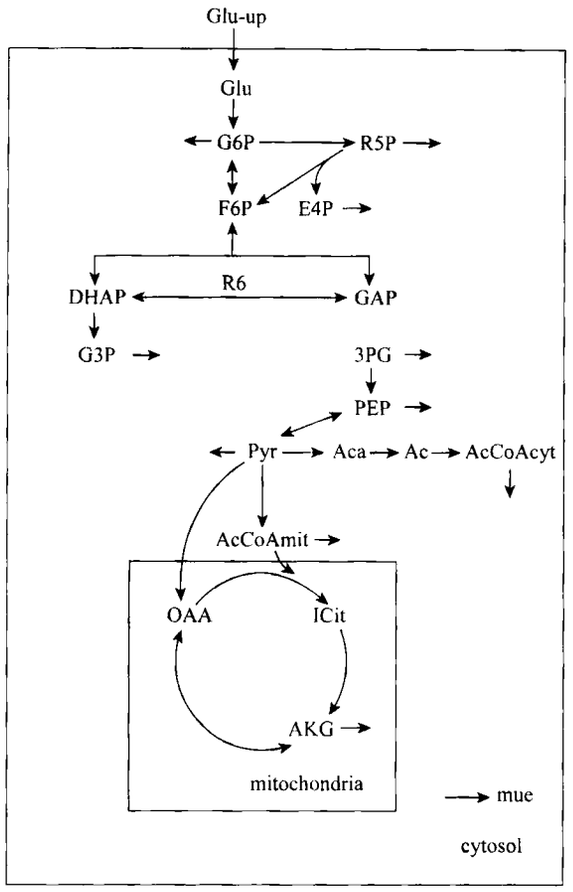

Figure 6 Graphical representation of the optimal biomass-producing EFM

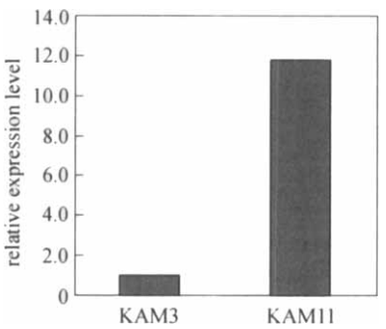

Figure 7 Real-time RT-PCR analysis of gene *GLT1* in strains KAM3 and KAM11
(Relative expression levels were determined after normalizing data to that of *GLT1* wild type strain KAM3, which was set at 1.0)

Table 7 Description of the biomass-producing pathway yields

EFM pathway No.	Mode stoichiometry	Biomass yield①/$g \cdot g^{-1}$
2	0.120 Glu-up=0.1 biomass + 0.037 CO_2 + 0.088 Glyc-ex	0.118
45	0.120 Glu-up=0.1 biomass + 0.123 CO_2 + 0.059 Glyc-ex	0.118
64	0.084 Glu-up=0.1 biomass + 0.087 CO_2	0.167
68	0.076 Glu-up=0.1 biomass + 0.037 CO_2	0.187

① Based on grams of glucose consumed.

Table 8 Comparison of different *S. cerevisiae* strain yields under anaerobic batch fermentation on a defined medium [containing 20g·(L glucose)$^{-1}$]

Strains	μ_{max}/h^{-1}	$Y_{X/S}$/g·g^{-1}	$Y_{Eth/S}$/g·g^{-1}	$Y_{Glyc/S}$/g·g^{-1}	$Y_{Ac/s}$/g·g^{-1}	$Y_{Pyr/s}$/g·g^{-1}	VP①/g·L^{-1}·h^{-1}
KAM3	0.337	0.048	0.477	0.0213	0.00014	0.00009	0.507
KAM11	0.349	0.050	0.501	0.0171	0.0002	0.00011	0.541
KAM2	0.370	0.058	0.441	0.028	0.0004	0.00019	0.506

① Volumetric productivity.

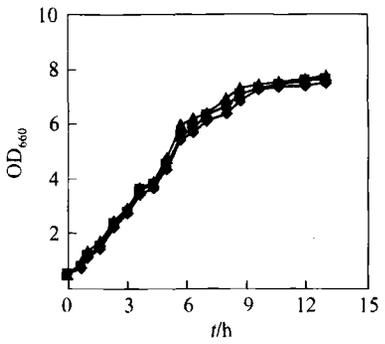

Figure 8 Growth curves of different strains on a defined medium in an anaerobic batch culture with an initial glucose concentration of 20 g·L^{-1}
▲ KAM2; ◆ KAM3; ■ KAM11

the predicted value of in silico simulation, possibly because of other physiological factors that affected biomass synthesis. The two engineered strains exhibited reduced production of pyruvate and acetate compared to the reference strain, which might also contribute to higher ethanol yields on account of the redirection of carbon flux towards ethanol formation. In addition, acetate was known as a potent inhibitor for ethanol fermentation. Thus, an increase in ethanol yield should be expected when the acetate yield of the genetically engineered strains decreased.

As described earlier, among the three yeast strains tested, the engineered strain KAM11 showed the highest ethanol yield. In addition, strain KAM11 was superior to strain KAM3 in terms of ethanol volumetric productivity and specific growth rate. This could be explained in two aspects: ① deletion of *FPS1*, resulting in the redirection of carbon flux from glycerol formation to ethanol production; ② overexpression of *GLT1* affected cofactor regulation positively, including improved NADH balance and enhanced ATP consumption, which induced a reprogramming of cellular metabolism in favor of anaerobic ethanol fermentation.

4 CONCLUSIONS

The fermentation performance of the engineered strains KAM3 and KAM11 agree very well with the calculated results of EFM analysis. It suggests that EFM analysis can be applied to design, to evaluate strategies of strain construction for optimal ethanol yield in *Saccharomyces cerevisiae*. Moreover, the metabolic network model used here is valid.

ACKNOWLEDGEMENTS

The authors honestly thank Dr. Hongwu Ma and Feng He at the German Research Center for Biotechnology for their meaningful suggestions on EFM analysis. This study was carried out under the supervision of Prof. Pingsheng Ma.

REFERENCES

1 van Dijken, J.P., Scheffers, W.A., "Redox balances in the metabolism of sugars by yeast", *FEMS Microbiol. Rev.*, **32**, 199-224 (1986).
2 Nevoigt, E., Stahl, U., "Osmoregulation and glycerol metabolism in the yeast *Saccharomyces cerevisiae*", *FEMS Microbiol. Rev.*, **21**, 231-241 (1997).
3 Bakker, B.M., Overkamp, K.M., Van Maris, A.J., Kötter, P., Luttik, M.A., van Dijken, J.P., Pronk, J.T., "Stoichiometry and compartmentation of NADH metabolism in *Saccharomyces cerevisiae*", *FEMS Microbiol. Rev.*, **25**, 15-37 (2001).
4 Hohmann, S., "Osmotic stress signaling and osmoadaptation in yeasts. Microbiol", *Mol. Biol. Rev.*, **66**, 300-372 (2002).
5 Michnick, S., Roustan, J.L., Remize, F., Barre, P., Dequin, S., "Modulation of glycerol and ethanol yields during alcoholic fermentation in *Saccharomyces cerevisiae* strains overexpressed or disrupted for *GPD1* encoding glycerol-3-phosphate dehydrogenase", *Yeast*, **13**, 783-793 (1997).
6 Valadi, H., Larsson, C., Gustafsson, L., "Improved ethanol production by glycerol-3-phosphate dehydrogenase mutants of *Saccharomyces cerevisiae*", *Appl. Microbiol. Biotechnol.*, **50**, 434-439 (1998).
7 Nissen, T.L., Hamann, C.W., Kielland-Brandt, M.C., Nielsen, J., Villadsen, J., "Anaerobic and aerobic batch cultivations of *Saccharomyces cerevisiae* mutants impaired in glycerol synthesis", *Yeast*, **16**, 463-474 (2000a).
8 Valenzuela, L., Ballario, P., Aranda, C., Filetici, P., Gonzalez, A., "Regulation of expression of *GLT1*, the gene encoding glutamate synthase in *Saccharomyces cerevisiae*", *J. Bacteriol.*, **180**, 3533-3540 (1998).
9 Nissen, T.L., Kielland-Brandt, M.C., Nielsen, J., Villadsen, J., "Optimization of ethanol production in *Saccharomyces cerevisiae* by metabolic engineering of the ammonium assimilation", *Metab. Eng.*, **2**, 69-77 (2000b).
10 Remize, F., Cambon, B., Barnavon, L., Dequin, S., "Glycerol formation during wine fermentation is mainly linked to Gpd1p and is only partially controlled by the HOG pathway", *Yeast*, **20**, 1243-1253 (2003).
11 Oliveira, R., Lages, F., Silva-Graça, M., Lucas, C., "Fps1p channel is the mediator of the major part of glycerol passive diffusion in *Saccharomyces cerevisiae*: Artefacts and re-definitions", *Biochim. Biophys. Acta.*, **1613**, 57-71 (2003).
12 Luyten, K., Albertyn, J., Skibbe, W.F., Prior, B.A., Ramos, J., Thevelein, J.M., Hohmann, S., "Fps1p, a yeast member of the MIP-family of channel proteins, is a facilitator for glycerol uptake and efflux and it is inactive under osmotic stress", *EMBO J.*, **14**, 1360-1371 (1995).
13 Tamás, M.J., Luyten, K., Sutherland, F.C., Hernandez, A., Albertyn, J., Valadi, H., Li, H., Prior, B.A., Kilian, S.G., Ramos, J., Gustafsson, L., Thevelein, J.M., Hohmann, S., "Fps1p controls the accumulation and release of the compatible solute glycerol in yeast osmoregulation", *Mol. Microbiol.*, **4**, 1087-1104 (1999).
14 Hedfalk, K., Bill, R.M., Jonathan, G.L., Mullins, G.L., Karlgren, S., Filipsson, C., Bergstrom, J., Tamás, M.J., Rydström, J., Hohmann, S.,

"A regulatory domain in the C-terminal extension of the yeast glycerol channel Fps1p", *J. Biol. Chem.*, **158**, 14954-14960 (2004).
15 Zhang, A.L., Kong, Q.X., Cao, L.M., Chen, X., "Effect of FPS1 deletion on the fermentation properties of *Saccharomyces cerevisiae*", *Lett. Appl. Microbiol.*, **44**, 212-217 (2007).
16 Förster, J., Famili, I., Fu, P., Palson, B.O., Nielsen, J., "Genome-scale reconstruction of the *Saccharomyces cerevisiae* metabolic network", *Genome Res.*, **13**, 244-253 (2003).
17 Duarte, N.C., Herrgard, M.J., Palsson, B.O., "Reconstruction and validation of *Saccharomyces cerevisiae* iND750, a fully compartmentalized genome-scale metabolic model", *Genome Res.*, **14**, 1298-1309 (2004).
18 Bro, C., Regenberg, B., Forster, J., Nielsen, J., "In silico aided metabolic engineering of *Saccharomyces cerevisiae* for improved bioethanol production", *Metab. Eng.*, **8**, 102-111 (2006).
19 Schuster, S., Fell, D., Dandekar, T., "A general definition of metabolic pathways useful for systematic organization and analysis of complex metabolic networks", *Nat. Biotechnol.*, **18**, 326-332 (2000).
20 Stephanopoulos, G., Alper, H., Moxley, J., "Exploiting biological complexity for strain improvement through systems biology", *Nat. Biotechnol.*, **22**, 1261-1267 (2004).
21 Schwartz, J.M., Kanehisa, M., "Quantitative elementary mode analysis of metabolic pathways: The example of yeast glycolysis", *BMC Bioinformatics*, **7**, 186 (2006).
22 Carlson, R., Fell, D., Srienc, F., "Metabolic pathway analysis of a recombinant yeast for rational strain development", *Biotechnol. Bioeng.*, **79**, 121-134 (2002).
23 Förster, J., Gombert, A.K., Nielsen, J.,"A functional genomics approach using metabolomics and *in silico* pathway analysis", *Biotechnol. Bioeng.*, **79**, 704-712 (2002).
24 Palsson, B.O., Price, N.D., Papin, J.A., "Development of network-based pathway definitions: The need to analyze real metabolic networks", *Trends Biotechnol.*, **21**, 195-198 (2003).
25 Çakır, T., Kırdar, B., Ülgen, K.Ö., "Metabolic pathway analysis of yeast strengthens the bridge between transcriptomics and metabolic networks", *Biotechnol. Bioeng.*, **86**, 251-260 (2004).
26 Klamt, S., Stelling, J., Ginkel, M., Gilles, E.D., "Flux analyzer: Exploring structure, pathways, and flux distributions in metabolic networks on interactive flux maps", *Bioinformatics*, **19** (2), 261-269 (2003).
27 Kong, Q.X., Cao, L.M., Zhang, A.L., Chen, X., Zhao, X.M., "Overexpression of *GLT1* in gpd1Δ mutant to improve the production of ethanol of *Saccharomyces cerevisiae*", *Appl. Microbiol. Biotechnol.*, **73** (6), 1382-1386 (2007).
28 Nissen, T.L., Schulze, U., Nielsen, J., Villadsen, J., "Flux distributions in anaerobic, glucose-limited continuous cultures of *Saccharomyces cerevisiae*", *Microbiology*, **143**, 203-218 (1997).
29 Gombert, A.K., Moreira dos Santos, M., Christensen, B., Nielsen, J., "Network identification and flux quantification in the central metabolism of *Saccharomyces cerevisiae* under different conditions of glucose repression", *J. Bacteriol.*, **183** (4), 1441-1451 (2001).
30 Stückrath, I., Lange, H.C., Kötter, P., van Gulik, W.M., Entian, K.D., Heijnen, J.J., "Characterization of null mutants of the glyoxylate cycle and gluconeogenic enzymes in *S. cerevisiae* through metabolic network modeling verified by chemostat cultivation", *Biotechnol. Bioeng.*, **77**, 61-72 (2002).
31 Price, N.D., Reed, J.L., Palsson, B.O., "Genome-scale models of microbial cells: Evaluating the consequences of constraints", *Nat. Rev. Microbiol.*, **2**, 886-897 (2004).
32 Ostergaard, S., Olsson, L., Nielsen, J., "Metabolic engineering of *Saccharomyces cerevisiae*. Microbiol", *Mol. Biol. Rev.*, **64**, 34-50 (2000).
33 Bideaux, C., Alfenore, S., Cameleyre, X., Molina-Jouve, C., Uribelarrea, J.L., Guillouet, S.E., "Minimization of glycerol production during the high-performance fed-batch ethanolic fermentation process in *Saccharomyces cerevisiae*, Using a metabolic model as a prediction tool", *Appl. Environ. Microbiol.*, **72**, 2134-2140 (2006).

APPENDIX

Metabolite abbreviations①

Aca	acetaldehyde
Ac	acetate
Ac-ex	secreted acetate
AcCoAcyt	acetyl-CoAcyt
AcCoAmit	acetyl-CoAmit
ADP	adenosine diphosphate
ATP	adenosine triphosphate
AKG	2-oxoglutarate
CO_2	carbon dioxide
CO_2-ex	secreted carbon dioxide
DHAP	dihydroxy-acetone phosphate
E4P	erythrose-4-phosphate
Eth	ethanol
Eth-ex	ethanol secreted
F6P	fructose-6-phosphate
FAD	oxidized flavine adenine dinucleotide
$FADH_2$	reduced flavine adenine dinucleotide
G6P	glucose-6-phosphate
GAP	glyceraldehyde-3-phosphate
Glu	glucose
Glu-up	glucose uptake
Glum	glutamine
Glut	glutamate
Glyc	glycerol
Glyc-ex	glycerol efflux
G3P	glycerol-3-phosphate
ICit	isocitrate
Mal	malate
mue	biomass
NH_4^+	NH_4^+
NH_4^+-up	NH_4^+ uptake
OAA	oxaloacetate
3PG	3-phospho-glycerate
PEP	phosphoenolpyruvate
Pyr	pyruvate
Succ	succinate
R5P	ribose-5-phosphate
NAD^+cyt	oxidized nicotinamide adenine dinucleotide cyt
NAD^+mit	oxidized nicotinamide adenine dinucleotide mit
$NADP^+$cyt	oxidized nicotinamide adenine dinucleotide phosphate cyt
$NADP^+$mit	oxidized nicotinamide adenine dinucleotide phosphate mit
NADHcyt	reduced nicotinamide adenine dinucleotide cyt
NADHmit	reduced nicotinamide adenine dinucleotide mit
NADPHcyt	reduced nicotinamide adenine dinucleotide phosphate cyt
NADPHmit	reduced nicotinamide adenine dinucleotide phosphate mit

Reaction abbreviations

ACO	aconitaten hydratase
ACS	acetyl-coenzyme A synthetase
ADH	alcohol dehydrogenase
ALD	cytosolic aldehyde dehydrogenase
ATPX	ATP maintenance
BPH	acetate permease
CIT	citrate synthase
CO_2X	CO_2 transport
ENO	enolase
ETHX	ethanol permeas
FBA	aldolase
FUM	fumarate hydratase
FPS	glycerol permease
GLK	glucokinase
GLN	glutamine synthase
GLT	glutamate synthase
GND	phosphogluconate dehydrogenase
GPD	glycerol-3-phosphate dehydrogenase
GPM	phosphoglycerate mutase
GPP	glycerol phophatase
HXK	hexokinase

① cytosol, cyt; mitochondria, mit

HXT	glucose permease
IDH	isocitrate ehydrogenase (NAD^+ mit-dependent)
IDP	isocitrate ehydrogenase ($NADP^+$ mit-dependent)
KGD	alpha-ketoglutarate dehydrogenase
LSC	succinate-CoA ligase
MDH	malate dehydrogenase
MEP	NH_4^+ permease
MUEX	biomass formation
PCK	phosphoenolpyruvate carboxykinase
PDA, PDB	pyruvate dehydrogenase
PDC	pyruvate decarboxylase
PFK	phosphofructokinase
PGI	glucose-6-phosphate isomerase
PGK	3-phosphoglycerate kinase
PYC	pyruvate carboxylase
PYK	pyruvate kinase
RKI	ribose 5-phosphate isomerase
RPE	ribulose-phosphate 3-epimerase
SDH	succinate dehydrogenase
SOL	6-phosphoglucono-lactonase
TAL	transaldolase
TDH	glyceraldehyde-3-phosphate dehydrogenase
TKL	transketolase
TPI	triosephosphate isomerase
ZWF	glucose-6-phosphate dehydrogenase

Stoichiometric reactions involved in the mathematical model

R1: *MUEX*

0.24 AcCoAcyt + 0.03 AcCoAmit + 2.54 ATP + 0.11 AKG + 0.03 E4P + 0.25 G6P + 0.01 G3P + 0.1 OAA + 0.06 3PG + 0.06 PEP + 0.18 Pyr + 0.03 R5P + 0.16 NAD^+cyt + 0.06 NAD^+mit + 0.9 NADPHcyt + 0.22 NADPHmit $\longrightarrow$ 1 mue

R2: *HXT1, HXT2*

Glu-up $\longrightarrow$ 1 Glu

R3: *HXK1, HXK2, GLK1*

1 Glu + 1 ATP $\longrightarrow$ 1 ADP + 1 G6P

R4: *PGI1*

1 G6P $\rightleftharpoons$ 1 F6P

R5: *PFK1, PFK2, FBA1*

1 ATP + 1 F6P $\rightleftharpoons$ 1 ADP + 1 DHAP + 1 GAP

R6: *TPI1*

1 DHAP $\rightleftharpoons$ 1 GAP

R7: *TDH1, PGK1*

1 ADP + 1 GAP + 1 NAD^+cyt $\rightleftharpoons$ 1 ATP + 1 3PG + 1 NADHcyt

R8: *GPM1, GPM2, ENO1*

1 3PG $\rightleftharpoons$ 1 PEP

R9: *PYK1, PYK2*

1 ADP + 1 PEP $\longrightarrow$ 1 ATP + 1 Pyr

R10: *PDC1, PDC5, PDC6*

1 Pyr $\longrightarrow$ 1 Aca + 1 CO_2

R11: *ADH1, ADH2, ADH4*

1 Aca + 1 NADHcyt $\longrightarrow$ 1 Eth + 1 NAD^+cyt

R12: *ETHX*

1 Eth $\longrightarrow$ 1 Eth-ex

R13: *ALD6*

1 Aca + 1 $NADP^+$cyt $\longrightarrow$ 1 Ac + 1 NADPHcyt

R14: *BPH1*

1 Ac $\longrightarrow$ 1 Ac-ex

R15: *ACS1, ACS2*

1 Ac + 2 ATP $\longrightarrow$ 1 AcCoAcyt + 2 ADP

R16: *GPD1, GPD2*

1 DHAP + 1 NADHcyt $\longrightarrow$ 1 G3P + 1 NAD^+cyt

R17: *GPP1, GPP2*

1 G3P $\longrightarrow$ 1 Glyc

R18: *FPS1*

1 Glyc $\rightleftharpoons$ 1 Glyc-ex

R19: *ZWF1, SOL1*

GND1, RKI1:

1 G6P + 2 $NADP^+$cyt $\longrightarrow$ 1 CO_2 + 1 R5P + 2 NADPHcyt

R20: *RPE1, TKL1, TAL1*

2 R5P $\longrightarrow$ 1 E4P + 1 F6P

R21: *TKI1, TKI2*

1 E4P + 1 R5P $\longrightarrow$ 1 F6P + 1 GAP

R22: *PDA1, PDB1*

1 Pyr + 1 NAD^+mit $\longrightarrow$ 1 AcCoAmit + 1 CO_2 + 1 NADHmit

R23: *PYC1, PYC2*

1 ATP + 1 CO_2 + 1 Pyr $\longrightarrow$ 1 ADP + 1 OAA

R24: *CIT1, CIT3, ACO1*

1 AcCoAmit + 1 OAA $\longrightarrow$ 1 ICit

R25: *IDH1*

1 ICit + 1 NAD^+mit $\longrightarrow$ 1 AKG + 1 CO_2 + 1 NADHmit

R26: *IDP1*

1 ICit + 1 $NADP^+$mit $\longrightarrow$ 1 AKG + 1 CO_2 + 1 NADPHmit

R27: *KGD1, KGD2, LSC1*

1 ADP + 1 AKG + 1 NAD^+mit $\rightleftharpoons$ 1 ATP + 1 CO_2 + 1 Succ + 1 NADHmit

R28: *SDH1, SDH2, FUM1*

1 FAD + 1 Succ $\rightleftharpoons$ 1 $FADH_2$ + 1 Mal

R29: *MDH1*

1 Mal + 1 NAD^+mit $\rightleftharpoons$ 1 OAA + 1 NADHmit

R30: *PCK1*

1 ATP + 1 OAA $\longrightarrow$ 1 ADP + 1 CO_2 + 1 PEP

R31: *MEP1*

1 ATP + 1 NH_4^+-up $\longrightarrow$ 1 ADP + 1 NH_4^+

R32: *GLT1*

1 AKG + 1 Glum + 1 NADHcyt $\longrightarrow$ 2 Glut + 1 NAD^+cyt

R33: *GLN1*

1 ATP + 1 NH_4^+ + 1 Glut $\longrightarrow$ 1 ADP + 1 Glum

R34: CO_2X

1 CO_2 $\longrightarrow$ 1 CO_2-ex

R35: *ATPX*

1 ATP $\longrightarrow$ 1 ADP